J Mater Sci (2008) 43:4042–4049
DOI 10.1007/s10853-007-2143-3

REES RAWLINGS FESTSCHRIFT

Processing and magnetic properties of metal-containing SiCN ceramic micro- and nano-composites

Ralf Hauser · Adel Francis · Ralf Theismann · Ralf Riedel

Received: 13 June 2007 / Accepted: 6 September 2007 / Published online: 3 April 2008

Abstract Owing to their excellent high temperature and oxidation resistance, non-oxide polymer-derived silicon-based ceramics are suitable for applications in hot and corrosive environments. The metal (Fe, Co)-containing pre-ceramic compounds combine the processability of organic polymers with the physical and chemical characteristics of the metallic component. In this study, we will introduce two different routes to embed metal particles in a SiCN ceramic matrix, derived from the commercially available polysilazane Ceraset®. (1). Mixing and milling of metal powders (Fe, Co) with pre-crosslinked polysilazane followed by pyrolysis at 1100 °C. (2). Chemical reaction between metal carbonyl compounds, namely $Fe(CO)_5$ and $Co_2(CO)_8$, with pure polyorganosilazane followed by pyrolysis at 1100 °C. Both synthetic routes will be discussed on two particular examples, iron- and cobalt-containing samples as well as their resulting different microstructures with respect to their magnetic properties. The phases and microstructures of the metal–SiCN composites were investigated in terms of X-ray diffraction (XRD), scanning electron microscopy (SEM) coupled with EDX, transmission electron microscopy (TEM), Fourier transform infrared spectroscopy (FTIR) and magnetometer. Upon annealing in argon at 1100 °C, the crosslinked polysilazane blended with iron powder possesses a high saturation magnetization of about ~57 emu/g and exhibits good ferromagnetic behaviour in comparison to the one blended with cobalt. The magnetic measurements were performed within the temperature range 65–300 K.

R. Hauser · R. Theismann · R. Riedel
Darmstadt University of Technology, Institute of Materials Science, Petersenstraße 23, 64287 Darmstadt, Germany

A. Francis (✉)
Central Metallurgical Research and Development Institute (CMRDI), P.O. Box 87, Helwan, Cairo, Egypt
e-mail: adel_francis@hotmail.com

R. Theismann
Institute of Nanotechnology, Forschungszentrum Karlsruhe, 76021 Karlsruhe, Germany

Introduction

Because of their processing advantages compared to ceramics and metals, metal organic polymeric materials have tremendous application potential in the areas of materials science, electronics and medicine. Among the organosilicon polymers that have been found to be useful precursors for silicon-based ceramics are the polyorganosilazanes [1–4]. This class of materials is the ideal precursor for ternary Si–C–N ceramics synthesized by controlled pyrolysis of the polymeric precursors referred to as polymer-derived ceramics (PDC).

Polymer-derived SiCN ceramics provide an attractive material system for MEMS in ultra-high temperature and hostile environment applications [5]. Incorporating magnetic materials (active fillers, e.g. Co and Fe) as the sensing or active element offers new capabilities and opens new markets within the information technology, automotive, electronic, space and instrumentation. With this technique, new types of ceramic materials for high-temperature applications can be processed at relatively low temperatures compared to traditional ceramic fabrication methods. Specifically, this development enables the production of novel ceramic composites via pyrolysis of the pre-ceramic polymer containing reactive or inert filler particles.

The formation of ceramic materials from pre-ceramic polymers with alternating Si–O, Si–NH or Si–N=C=N

units as the backbone structure has been the subject of intensive research over the past two decades [5–12]. However, it has been recognized that the microstructure and the homogeneity of the as-synthesized SiCN ceramic composites can be influenced by the particle size and the reactivity of the inserted metal powders. Due to their high sensitivity against oxygen and moisture, it is difficult to use nano-sized metal powders as a filler to the ceramic composite. An alternative method to the nano powders is the application of molecular low valent metal compounds such as metal carbonyl compounds. These metal carbonyls can be distributed on a molecular level in the pre-ceramic polymer and are simpler to handle as related to metal nanopowders [13]. The thermal decomposition of $Co_4(CO)_{12}$ in the presence of methylene chloride in an autoclave leads to cobalt–carbon nano-cluster magnets embedded in amorphous carbon matrices [14]. Another synthetic route to highly distributed metal particles is the thermolytic decomposition of poly(ferrocenylsilanes) that leads to the formation of iron nano-particles embedded in an amorphous matrix [15]. Saha et al. [16] have synthesized SiCN composites with magnetic properties by mixing liquid polysilazane Ceraset® with 70 vol.% Fe_3O_4 particles and subsequently pyrolysis. They also showed that the magnetic behaviour of the samples depends on the pyrolysis temperature. Yan et al. [17] mixed different metal elements and alloys (Fe, Mn, Co, Ni, Ni–Mn, Co–Mn, Fe–Mn) with pre-crosslinked Ceraset® and found that the composites showed good soft magnetic properties. MacLachlan et al. [18] indicated that the magnetic properties of the shaped ceramic, synthesized by thermal polymerization of a metal-containing organosilicon monomer, could be tuned between a superparamagnetic and a ferromagnetic state by controlling the pyrolysis conditions. The magnetic properties were found to depend on the size of the iron nano-clusters homogeneously dispersed throughout the carbosilane–graphitic–silicon nitride matrix.

As developments in the field of magnetic materials are promising for future applications, the objective in this study is to analyse the magnetic properties of this composite material in relation to its microstructure, which in turn is a function of the preparation route and the annealing temperature.

Experimental procedure

The polymer precursor used in this work is a commercially available polysilazane, Ceraset® (Kion Inc. USA). It is a liquid sensitive to moisture and oxygen. Therefore a polysilazane polymer was manipulated and stored in a glove box under argon of 99.999% purity (Mbraun, Germany). The polysilazane was filled into a quartz tube and pyrolysed in a vertical quartz tube furnace with SiC heating elements (Fa. GERO, Germany). Thermal gravimetric analysis and characterization of this polymer have already been described elsewhere [7, 9, 11, 19]. Elemental Fe and Co (Alfa Aesar Co.) powders with a purity of 99.9% or better and a particle size of 10 μm and 45 μm, respectively, were used to form a microcomposite with the Ceraset®. The powders were mixed with the pre-crosslinked Ceraset® to give the desired composition. As metal carbonyl compounds we used $Fe(CO)_5$ and $Co_2(CO)_8$ from Fluka, Germany. Two different routes have been performed to embed metal particles in a SiCN matrix derived from the commercially available polysilazane Ceraset® (Kion Inc. USA):

(1) Mixing and milling of metal powders with pre-crosslinked polysilazane and subsequent pyrolysis according to the concept of "Active Filler Controlled Pyrolysis" [12, 20].

To synthesize the metal-based ceramics, the liquid polysilazane Ceraset® was pre-crosslinked at 280 °C in flowing argon, ground and ball milled in a planetary mill. The powder was sieved and the fraction <63 μm was used to produce compacts. The respective metal powder (1, 10 vol.% Fe and 10 vol.% Co) was added to Ceraset® and the mixture was homogenized by ball milling. The subsequent warm pressing process was performed at a pressure of 80 MPa at 300 °C with a holding time of 30 min.

(2) Chemical reaction between metal carbonyl compounds with pure polysilazane followed by polymer-to-ceramic transformation.

The preparation of the metal carbonyl based ceramics starts with the treatment of the pure polysilazane with the metal carbonyls in argon atmosphere without the addition of any solvents.

(a) Co: 2.0 g $Co_2(CO)_8$ (equivalent to 0.8 vol.% Co) was added to 10 mL Ceraset® in an ice bath. The reaction starts immediately with the release of gas and warming up of the mixture. After one h the reaction stopped and the evaporated materials were removed under vacuum, and the black solid residue was milled and warm pressed at 80 MPa and 180 °C with holding time of 30 min.

(b) Fe: 0.1 mL (0.7 g) $Fe(CO)_5$ (equivalent to 1.0 vol.% Fe) were added to 10 mL Ceraset®, mixed and heated at 60 °C for one h. The formation of a brown solid was noted, which was milled and warm pressed at 80 MPa and 180 °C with a holding time of 30 min.

All the samples were annealed at 1100 °C for 5 h under flowing argon in a quartz glass tube furnace. The processing procedure for the preparation of both metal-powder- and metal-carbonyl-based materials is shown in Fig. 1.

For the analysis of crystalline phases in the pyrolytic products, X-ray powder diffraction (XRD) studies were carried out on a STOE STADI-P with Mo Kα1 radiation in transmission. Diffraction data have been analysed by the Rietvelt method using the WinPLOTR package [21]. The overall microstructure characterization of the polymer-derived materials after pyrolysis and subsequent annealing was performed using high-resolution scanning electron microscopy (HRSEM) coupled with EDX (Philips XL 30 FEG with EDAX CDU LEAP detector). Additional microstructure characterization was performed by transmission electron microscopy (TEM) employing a JEOL JEM-3010 equipped with a Gatan Imaging Filter (GIF). IR spectra were measured with a Perking Elmer 1750 FT-IR spectrometer using an ATR-unit. FTIR transmission spectra of the matrix samples were recorded in the region of 500–4000 cm^{-1} at a resolution of 0.2 cm^{-1}. Chemical analyses of carbon, nitrogen and oxygen were carried out using Leco Instrumente GMBH C-200 (carbon analyser) and TC-436 (nitrogen and oxygen analysis). The iron and cobalt metal analysis was done at the Mikroanalytisches Labor Pascher (Remagen, Bandorf-Germany). Silicon contents were calculated so that the total of analysed fractions plus silicon reaches 100%. In addition, magnetic properties are taken in to account to evaluate the qualities of these materials. The magnetic properties of selected samples were determined using an LDJ Vibrating Sample Magnetometer (VSM, Model 9600) at room and liquid nitrogen temperature with a field up to 5000 Oersted (Oe). The magnetization values were normalized by the sample weight using the magnetic moment per gram (emu/g) as magnetization unit.

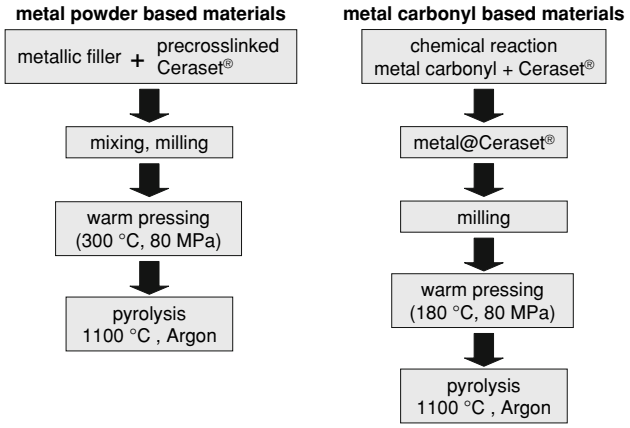

Fig. 1 Scheme of preparation of metal powder/SiCN and metal carbonyl/SiCN

Results and discussion

In our investigation related to the synthesis of polymer-derived SiCN-based ceramics with magnetic properties we modified the SiCN matrix by the addition of Fe or Co. The modification was done by two different routes: (i) Addition of metal particles to crosslinked polysilazane and (ii) reaction of polyorganosilazane with metal carbonyl compounds.

The chemical reaction between the carbonyl compounds and the pure polysilazane proceeds under cleavage of the CO groups and the formation of carbon monoxide. Cobalt carbonyl reacts with Ceraset® with a violent gas formation to form a black solid residue. In contrast, iron carbonyl does not react with Ceraset® at room temperature and needs heating up to 60 °C. After an h at this temperature, release of gas and formation of a brown solid residue were observed. Infrared spectroscopic investigations of the pure pre-crosslinked polymer as well as of the products of the reaction between the carbonyls and the pure polymer showed that in case of the cobalt-containing material, no *v*-CO-vibrations were observed within the region 2100–1700 cm^{1} (Fig. 2a). After reaction at 60 °C, the iron-containing sample shows a *v*-CO-vibration mode at 1990 cm^{-1} (Fig. 2b). These findings suggest the presence of bridged carbonyl groups connected to the iron atoms [22]. After the warm pressing process, all carbonyl bands disappeared.

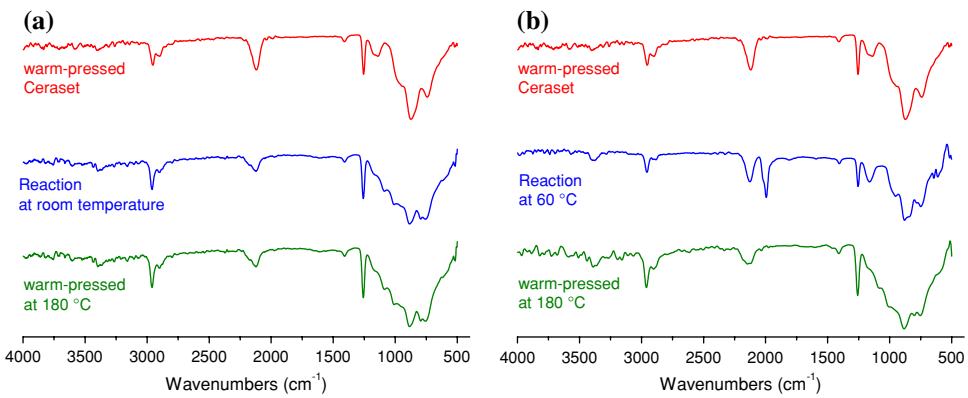

Fig. 2 IR spectra of the cobalt carbonyl-(**a**) and iron carbonyl-derived samples (**b**) in comparison to the pure warm pressed Ceraset®

A comparison of the ratio between the C–H vibration modes at around 3000 cm^{-1} and the vibration modes for the Si–H bonds in the pure crosslinked Ceraset® and the carbonyl-treated materials clearly shows a reduction of the Si–H bonds at 2100 cm^{-1} in the metal carbonyl-treated compounds. This feature indicates that the process of crosslinking of the polysilazane Ceraset® follows a dehydrocoupling mechanism catalysed by the metal carbonyls. The metal carbonyl compounds are decomposed during this process and form metal clusters under cleavage of carbon monoxide during this reaction [23–25].

It was expected that the pyrolytic conversion of polysilazanes blended with cobalt or iron leads to the formation of the respective metal nitride or carbide particles. However, the XRD pattern of the as-prepared iron-containing polymer pyrolysed at 1100 °C for 5 h under argon atmosphere (Fig. 3a) shows well-defined peaks characteristic for Fe_3Si (spacegroup: Fm-3m; a = 5.696(1) Å). The XRD obtained from the cobalt-containing sample exhibits peaks characteristic for Co_2Si (spacegroup: Pnam; a = 4.934(2) Å; b = 7.136(2) Å; 3.755(1) Å) (Fig. 4a). These findings are consistent with the work of Corriu et al. [23] who observed products such as mixed $Fe_xSi_yC_z$ phases or Co_2Si instead of metallic nano-particles as a result of the thermolysis of ferrocyne containing organosilicon diacetylene oligomers with one of the triple bonds complexed with dicobalt hexacarbonyl. Other authors [24] detected crystalline Fe_3Si and Co_2Si from the reactions of 2,5-dis ilahexane with cobalt- or iron carbonyl as well as the formation of metal-rich nodules in a homogeneous matrix for the samples pyrolysed at 1000 °C. It was not possible to refine the XRD pattern of the carbonyl-based materials. The amorphous nature is demonstrated by the absence of any well-defined diffraction peaks (Figs. 3b and 4b). The only peak in the diffraction pattern of the iron carbonyl-based material belongs to the 220 reflex of $FeSi_3$ with a d value of $d = 2{,}0138$ and a calculated crystallite size of 3.5 nm. This result gives a hint of the formation of Fe_3Si and Co_2Si and is in good agreement with the results from the TEM investigations mentioned below. Even though the X-ray diffraction pattern from these materials is almost featureless, they are not strictly amorphous. They contain short-range structural features, which we call nano-domains. It is likely that the nature of the nano-domains is the basis for the remarkable resistance of PDCs to crystallization even at ultra-high temperatures [26].

To obtain an estimate of the pyrolysed samples' composition, a series of elemental analyses were conducted. Table 1 shows that oxygen contents in the metal carbonyl-based materials are much higher than oxygen contents of the metal powder-based materials. This might be due to the rapid oxidation of fine metal particles. The results also

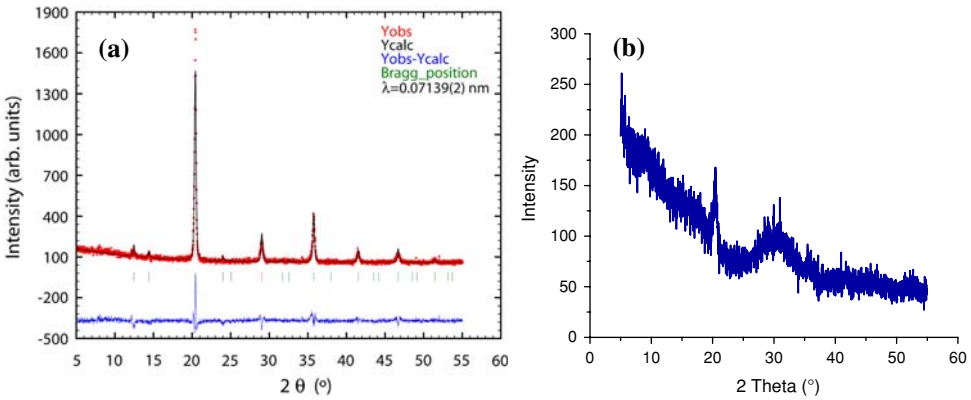

Fig. 3 XRD pattern of the iron-containing samples, (**a**) metal powder (observed and calculated diffraction profiles together with their difference curve, $FeSi_3$), (**b**) iron carbonyl

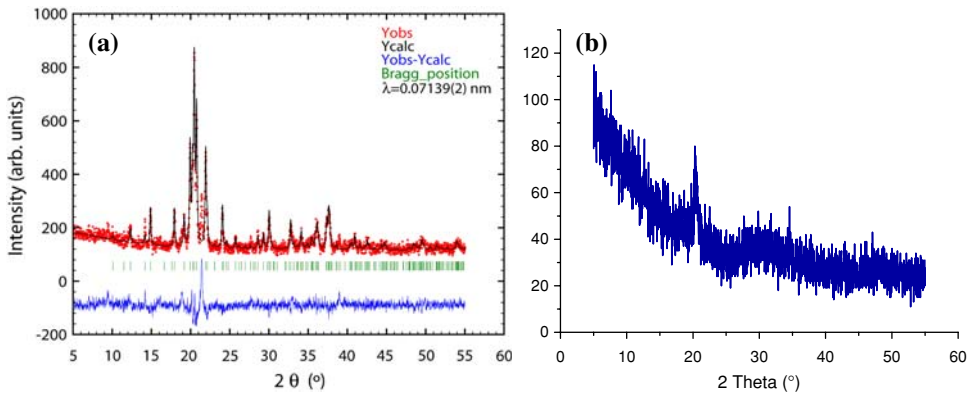

Fig. 4 XRD pattern of the cobalt-containing samples, (**a**) metal powder (observed and calculated diffraction profiles together with their difference curve, $CoSi_2$), (**b**) cobalt carbonyl

showed a variation of the iron content as a function of the preparation route which is consistent with the XRD results where Fe_3Si is found as the main crystalline phase.

Figure 5 represents SEM images of the microstructure of the iron-containing SiCN ceramics. The metal powder-based material exhibits a clear-cut area division in iron-rich (bright) and iron-poor (dark) areas where the iron particles are homogeneously dispersed in the whole matrix. A grain structure similar to the iron particles used as starting substance is not observable. This leads to the conclusion that the observed microstructure is a result of chemical reactions and transport processes during the polymer to ceramic transformation. In contrast, the iron carbonyl-based ceramic does not show any phase separation even at higher magnification. SEM micrograph of samples filled with 1 vol.% iron powder is illustrated in Fig. 6. This picture demonstrates that the low amount of iron powder did not lead to a homogeneous distribution of iron in the SiCN matrix. An explanation of the homogeneity of the metal carbonyl-based ceramics is the molecular distribution of the carbonyl compounds in the pre-ceramic polymer and their subsequent chemical reaction with it by cleavage of carbon monoxide. To investigate the microstructure of the metal carbonyl-derived materials, TEM technique was used. The TEM image and the results of the Fe-elemental-mapping are presented in Fig. 7 where iron enriched nano-particles with a diameter of 5 nm were found, embedded in an amorphous matrix. In such nano-particles, lattice fringes could be observed with a distance of 2.02(5) Å (Fig. 7a),

Table 1 Elemental composition of pyrolysed Ceraset® samples

Pyrolysed samples	Elemental composition in wt%					
	Si	C	N	O	Fe	Co
Ceraset® + 10 vol.% Fe	27.06	9.85	7.73	1.11	54.25	–
Ceraset® + 10 vol.% Co	16.04	8.98	8.3	1.63	–	56.05
Ceraset® + 1 vol.% $Fe(CO)_5$	61.2	17.2	15.29	3.67	2.64	–
Ceraset® + 1 vol.% $Co_2(CO)_8$	50.79	17.42	16.7	8.67	–	6.42

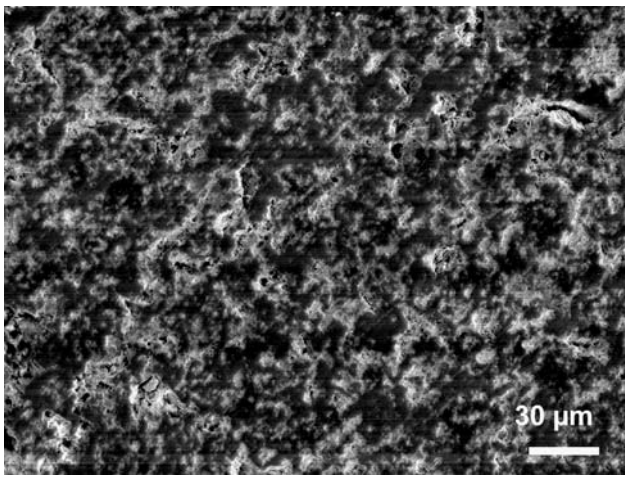

Fig. 6 SEM image of an iron metal powder derived sample, containing 1 vol.% iron powder

which can be attributed to the 220 lattice plane of iron silicide in agreement with the X-ray data. The cobalt-containing ceramic showed the same principal behaviour as the iron-filled material. The microstructure presented in the SEM micrographs is also subdivided into cobalt-rich (bright) and cobalt-poor (dark) zones. Also in this case the grain structure of metal powder does not remain. The homogeneity of the carbonyl-based sample is demonstrated in the SEM images on the right in Fig. 8.

The magnetization vs. applied field for the annealed Ceraset®-iron powder and iron carbonyl is shown in Fig. 9a and b, respectively, as investigated by vibrating sample magnetometer (VSM). The specific saturation magnetization M_s and coercivity H_c are calculated for the different ferromagnetic compositions of the samples. The hysteresis loops for the three samples at different temperatures ranging from 65 to 300 K were characterized by a narrow area, with small values of coercivity and remanence. Because of the crystalline nature of the compound, Fe_3Si and the amount of vol.% Fe added, higher saturation magnetizations were observed in Fig. 9a than those in Fig. 9b. In the former, the saturation magnetization was almost constant ~57 emu/g while a decrease in coercivity

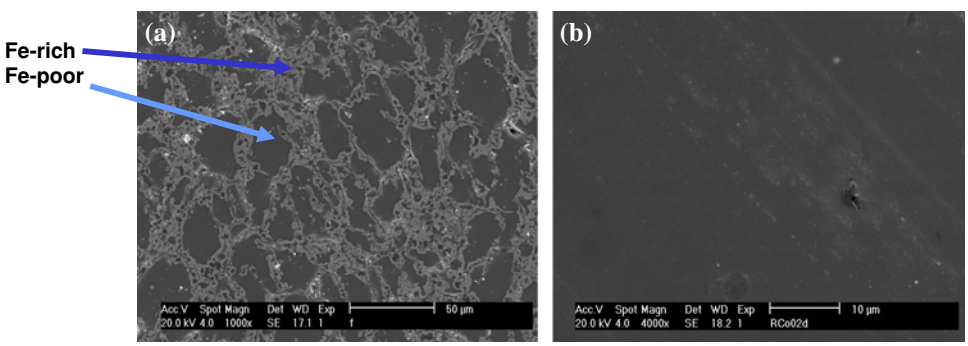

Fig. 5 SEM images of the iron-containing samples, (**a**) metal powder and (**b**) iron carbonyl

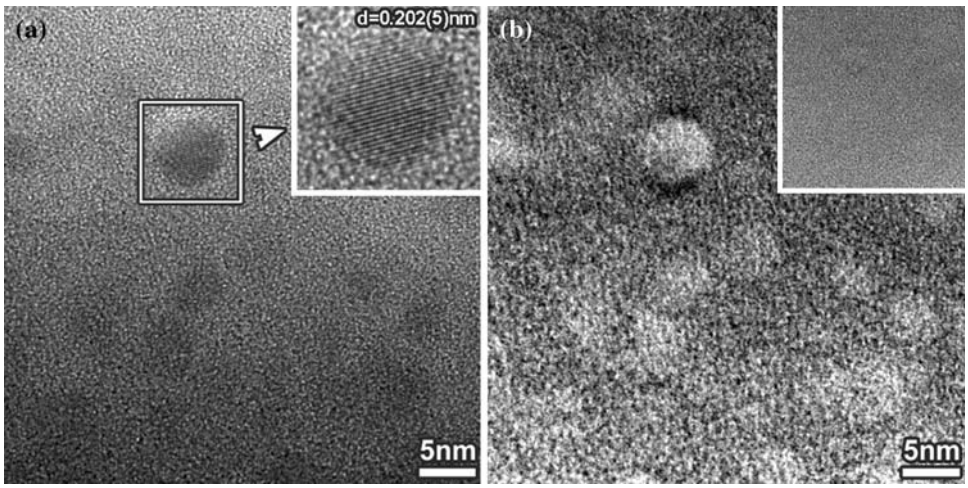

Fig. 7 (**a**) HR-TEM image of the iron carbonyl-derived sample, the *d*-spacing of 0.202(5) nm of the magnified particle (inset upper right) can be attributed to the Fe_3Si 220 reflection. (**b**) iron map from the same area obtained with the three-window method, iron-enriched areas are shown bright. The inset shows the jump-ratio image of the two pre-edge images to demonstrate the absence of any diffraction contrast

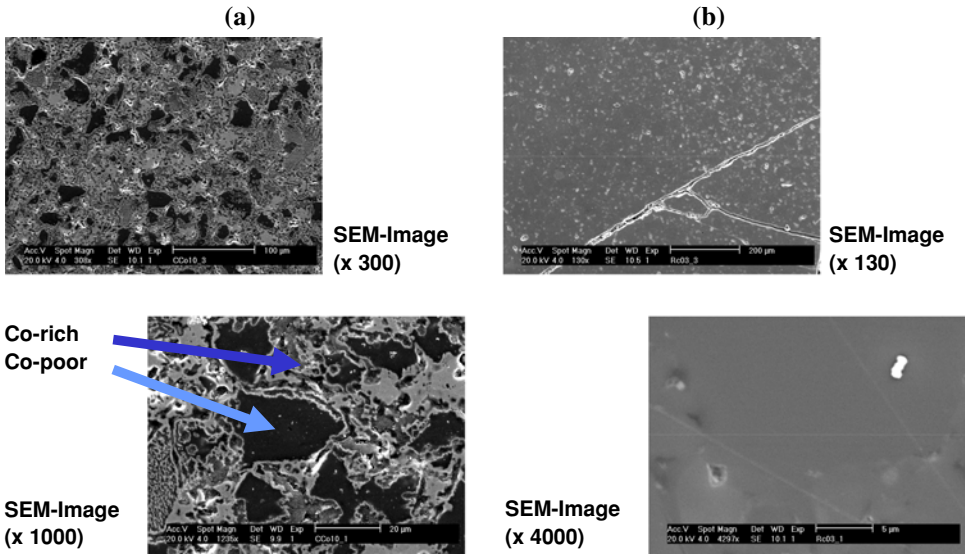

Fig. 8 SEM images of the cobalt-containing samples, (**a**) metal powder and (**b**) cobalt carbonyl

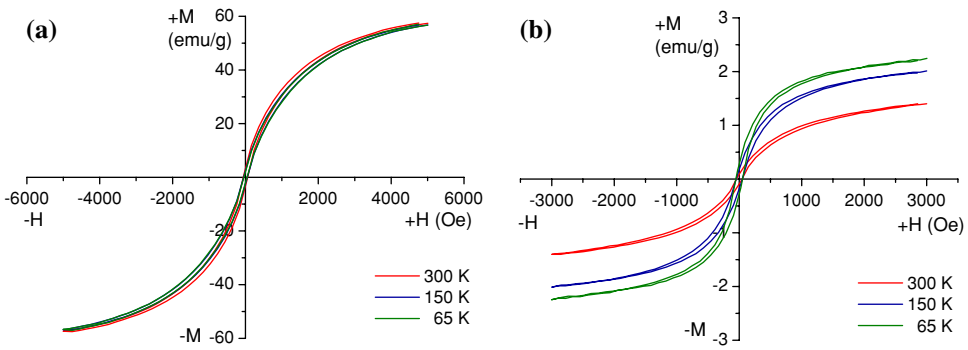

Fig. 9 Magnetization vs. field measurements for iron-containing ceraset samples prepared at 1100 °C (at 65–300 K). The hysteresis curves demonstrate the magnetic homogeneity of the material. (**a**) blended metal powder (**b**) iron carbonyl

from 60 Oersted (Oe) to 42 Oe was observed as we go down under 300 K. It should be noted that the iron-ceraset samples showed a definite hysteresis loop at both room and liquid nitrogen temperature. The coercive force of iron-doped or carbonyl samples did not show significant difference. It is interesting to observe that the saturation magnetization (M_s) was higher for iron powder samples than iron carbonyl samples. The difference in the magnetic behaviour might be explained by the different stoichiometries or compositions as due to the interaction of the magnetic moments in the Fe/Ceraset®-composite. This feature also suggests that the shell layer consists of several aggregated iron particles of larger size as demonstrated in Fig. 5 and the surface effects can modify the saturation

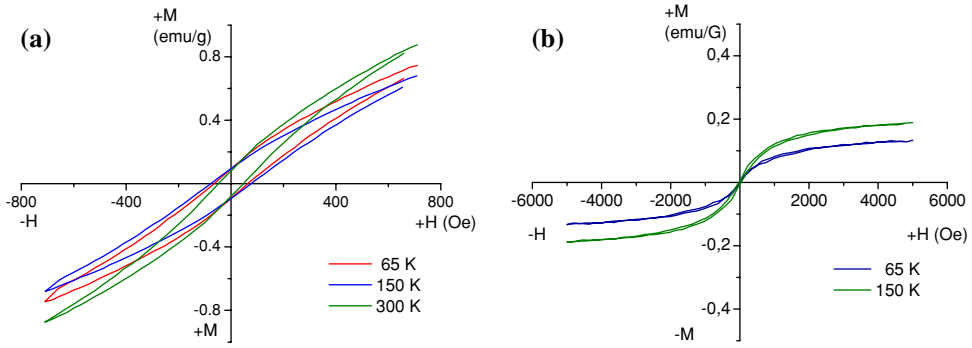

Fig. 10 Magnetization versus field measurements for cobalt-containing ceraset samples prepared at 1100 °C (at 65–300 K). (**a**) metal powder (**b**) cobalt carbonyl

magnetization of the magnetic material. The compositional, thermal and microstructural variations of hysteresis parameters like Ms, Hc and Mr/Ms reveal that grains in the compositions investigated are of multidomain (M-D) type. As we suggested, the ferromagnetic phase (FM) observed in the samples is ascribed to Fe_3Si phase formed during the pyrolysis process. The higher fraction of 10 vol.% Fe particles with respect to that of 1 vol.% of Fe-pentacarbonyl results in an increased Ms. In the composites containing 1 and 10 vol.% Fe particles Fe-rich segregations can be found after pyrolysis by SEM (Figs. 5a, 6). In contrast in the Fe-pentacarbonyl-derived sample no such segregations can be analysed (see Fig. 5b).

Magnetization measurements of the annealed Ceraset®-cobalt powder and cobalt carbonyl (Fig. 10a, b) showed virtually no good hysteresis. The blended cobalt powder with ceraset is slightly better than the carbonyl counterpart. However, the ceramic prepared at this temperature rapidly reached saturation (Fig. 10b) and displayed hysteresis with a small remanence in its magnetization. By varying the pyrolysis temperature and annealing time of the pre-cer amic polymer blended with Co, we can control the magnetic properties of the resulting ceramic.

In our work, emphasis is placed on the unique magnetic properties created through material processing of polymer-derived ceramics. Further experiments are required, however, to assess quantitatively the dependence of the magnetic properties on the magnetic phase content embedded in the polyorganosilazane. It is also necessary to investigate if enhanced soft magnetic or unique magnetic behaviour can be achieved by adjusting the annealing and crystallization conditions. A more detailed investigation regarding the influence of other additives is the focus of an on-going study.

In general, the PDC route could be considered as a practical and an excellent alternative among the various processing techniques (e.g. hot pressing, thermal or plasma spray, mechanical alloying, variants of reactive sintering) to produce silicide alloys and their composites. The thermal conversion of modified pre-ceramic polymers such as Ceraset® results in the in situ formation of transition metal silicides at rather low temperatures. Furthermore, new functional magnetic properties of SiCN-based ceramics are obtained by this in situ formation of metal silicides.

Conclusions

SiCN ceramics with magnetic properties can be synthesized by mixing a metallic filler powder with pre-crosslinked polysilazanes or by chemical reaction of the pure silazane with low valent metal carbonyl compounds. The homogeneity of the samples and the size of the metal-containing particles are strongly dependent on size and reactivity of the filler systems. Metal powders lead to the formation of micrometer-sized particles. Metal-containing nano-particles were formed in the carbonyl-derived materials. All samples show soft magnetic properties, the value of magnetization and the coercive field depends on the amount of magnetic particles and their distribution in the polymer-derived ceramic matrix. To determine the nature of the domain states existing in our Si–C–N system, we summarized the data related to thermal variation of hysteresis parameters as follows:

(1) The hysteresis loops of all the compositions investigated are narrow.
(2) The shape of the loop does not change appreciably with temperature from 300 to 65 K.
(3) The remanence ratio Mr/Ms of all the compositions is less than 0.15 and does not vary significantly with temperature.
(4) The coercive force is small and almost temperature independent.

All the above observations strongly support the presence of multidomain (M-D) grains in the PDC composites investigated in this study.

Acknowledgements A. F., who spent 2 months at the Technische Universität Darmstadt (TUD) under the sponsorship of the DAAD fellowship programme, acknowledges the support of the DAAD. Furthermore, A. F. is grateful to the Alexander von Humboldt

Foundation for the Georg-Forster research fellowship. R.R. extends his gratitude for the financial support of the Fonds der Chemischen Industrie, Frankfurt, Germany.

References

1. Riedel R, Kienzle A, Friess M (1995) In: Harrod JF, Laine RM (eds) Applications of organo-metallic chemistry in the preparation and processing of advanced materials. Kluwer Academic Publishers, The Netherlands, pp 155
2. Bill J, Aldinger F (1995) Adv Mater 7(9):775
3. Seyferth D (1991) In: Ziegler G, Hausner H (eds) Euro-ceramics 2: vol. 1, The proceedings of the second European ceramic society conference (Ecers '91). FRGDeutsche Keramishe Gesellscheft e.V.: Augsburg, p 567
4. Narula CK (1995) Ceramic precursor technology and its applications. Marcel Dekker Inc., USA, pp 83
5. Liew L, Zhang W, An L, Shah S, Luo R, Lui Y, Dunn ML, Bright V, Raj R, Anseth K (2001) Am Cer Soc Bull 80(5):25
6. An L, Riedel R, Konetschny C, Kleebe H-J, Raj R (1998) J Am Ceram Soc 81:1349
7. An L, Wang Y, Bharadwaj L, Fan Y, Zhang L, Jiang D, Sohn Y, Desai VH, Kapat J, Chow LC (2004) Adv Eng Mat 6(5):337
8. Raj R, An L, Shah S, Riedel R, Fasel C, Kleebe H-J (2001) J Am Ceram Soc 84(8):1803
9. Iwamoto Y, Völger W, Kroke E, Riedel R (2001) J Am Ceram Soc 84(10):2170
10. Riedel R, Kienzle A, Dreßler W, Ruwisch L, Bill J, Aldinger F (1996) Nature 382:796
11. Haluschka C, Engel C, Riedel R (2000) J Eur Ceram Soc 20:1365
12. Greil P (1998) J Eur Ceram Soc 18(13):1905
13. Tsirlin AM, Shcherbakova GI, Florina EK, Popova NA, Gubin SP, Moroz EM, Riedel R, Kroke E, Steen M (2002) J Eur Ceram Soc 22:2577
14. Nishi N, Kosugi K, Hino K, Yokoya T, Okunishi E (2003) Chem Phys Lett 369:198
15. Kulbaba K, Resendes R, Cheng A, Bartole A, Safa-Sefat A, Coombs N, Stover HDH, Greedan JE, Ozin G, Manners I (2001) Adv Mater 13:732
16. Saha A, Shah SR, Raj R, Russek SE (2003) J Mater Res 18(11):2549
17. Yan X, Cheng X, Li C, Hauser R, Riedel R (2007) Mat Sci Forum 546–549:2269
18. MacLachlan M, Ginzburg M, l Coombs N, Coyle TW, Raju NP, Greedan JE, Ozin GA, Manners I (2000) Science 287:1460
19. Riedel R, Mera G, Hauser R, Klonczynski A (2006) J Ceram Soc Japan 114(6):425
20. Greil P (1995) J Am Ceram Soc 78:835
21. Roisnel T, Rodrigues-Carvajal J (2001) Mat Sci Forum 378:118
22. (a) Keeley DF, Johnson RE (1959) J Inorg Nucl Chem 11:33 (b) King RB, Stone FGA (1963) Inorg Synt 7:193
23. Corriu RJP, Devylder N, Guerin C, Henner B, Jean A (1996) J Organomet Chem 509:249
24. Bourg S, Boury B, Corriu RJP (1998) J Mater Chem 8(4):1001
25. Li Y-L, Kroke E, Riedel R, Fasel C, Gervais C, Babonneau F (2001) Appl Organomet Chem 15:820
26. Riedel R, Passing G, Schönfelder H, Brook RJ (1992) Nature 355:714